Hamiltonian Cycles in Linear-Convex Supergrid Graphs

Ruo-Wei Hung
Department of Computer Science and Information Engineering,
Chaoyang University of Technology,
Wufeng, Taichung 41349, Taiwan
E-mail: rwhung@cyut.edu.tw

June 2, 2015

arXiv:1506.00190v1 [cs.DM] 31 May 2015

Abstract

A supergrid graph is a finite induced subgraph of the infinite graph associated with the two-dimensional supergrid. The supergrid graphs contain grid graphs and triangular grid graphs as subgraphs. The Hamiltonian cycle problem for grid and triangular grid graphs was known to be NP-complete. In the past, we have shown that the Hamiltonian cycle problem for supergrid graphs is also NP-complete. The Hamiltonian cycle problem on supergrid graphs can be applied to control the stitching trace of computerized sewing machines. In this paper, we will study the Hamiltonian cycle property of linear-convex supergrid graphs which form a subclass of supergrid graphs. A connected graph is called k-connected if there are k vertex-disjoint paths between every pair of vertices, and is called locally connected if the neighbors of each vertex in it form a connected subgraph. In this paper, we first show that any 2-connected, linear-convex supergrid graph is locally connected. We then prove that any 2-connected, linear-convex supergrid graph contains a Hamiltonian cycle.

Keywords: Hamiltonian cycle, locally connected, linear-convex supergrid graph, supergrid graph, grid graph, triangular grid graph, computer sewing machine

1 Introduction

A *Hamiltonian cycle* in a graph is a simple cycle in which each vertex of the graph appears exactly once. The *Hamiltonian cycle* problem involves determining whether or not a graph contains a Hamiltonian cycle. A graph is said to be *Hamiltonian* if it contains a Hamiltonian cycle. The Hamiltonian path problem is defined similarly. They have numerous applications in different areas, including establishing transport routes, production launching, the on-line optimization of flexible manufacturing systems [1], computing the perceptual boundaries of dot patterns [29], pattern recognition [2, 30, 33], and DNA physical mapping [14]. It is well known that the Hamiltonian problems are NP-complete for general graphs [10, 21]. The same holds true for bipartite graphs [24], split graphs [11], circle graphs [7], undirected path graphs [3], planar bipartite graphs with maximum degree 3 [20], grid graphs [20], triangular grid graphs [12], and supergrid graphs [18].

Let G be a graph with the vertex set $V(G)$ and edge set $E(G)$. Graph G is *connected* if there exists a path between every pair of its vertices, and G is called k-connected ($k \geqslant 2$) if there are k vertex-disjoint paths between every pair of vertices in G. Obviously, if graph G is not 2-connected, then G contains no Hamiltonian cycle. In addition, a 2-connected graph does not imply that it is Hamiltonian. For each vertex v of G, the *neighborhood* $N(v)$ of v is the set of all vertices adjacent to v. For a subset of vertices $S \subseteq V(G)$, the subgraph of G induced by S is denoted by $G[S]$. A vertex v of G is said to be *locally connected* if $G[N(v)]$ is connected. Graph G is called *locally connected* if each vertex of G is locally connected. The locally connected property of graphs can be applied to VLSI architecture [15]. Some further survey for local connectivity can be found in [9].

The *two-dimensional integer grid* G^∞ is an infinite graph whose vertex set consists of all points of the Euclidean plane with integer coordinates and in which two vertices are adjacent if and only if the (Euclidean) distance between them is equal to 1. The *two-dimensional triangular grid* T^∞ is an infinite graph obtained from G^∞ by adding all edges on the lines traced from up-left to down-right. A fragment of graph G^∞ and T^∞ is depicted in Fig. 1(a) and Fig. 1(b), respectively. A *grid graph* is a finite, vertex-induced subgraph of G^∞. For a node v in the plane with integer coordinates, let v_x and v_y be the x and y *coordinates* of node v, respectively, denoted by $v = (v_x, v_y)$. If v is a vertex in a grid graph, then its possible neighbor vertices include $(v_x, v_y - 1)$, $(v_x - 1, v_y)$, $(v_x + 1, v_y)$, and $(v_x, v_y + 1)$. For example, Fig. 2(a) shows a grid graph. A *triangular grid graph* is a finite, vertex-induced subgraph of T^∞. If v is a vertex in a triangular grid graph, then its possible neighbor vertices include $(v_x, v_y - 1)$, $(v_x - 1, v_y)$, $(v_x + 1, v_y)$,

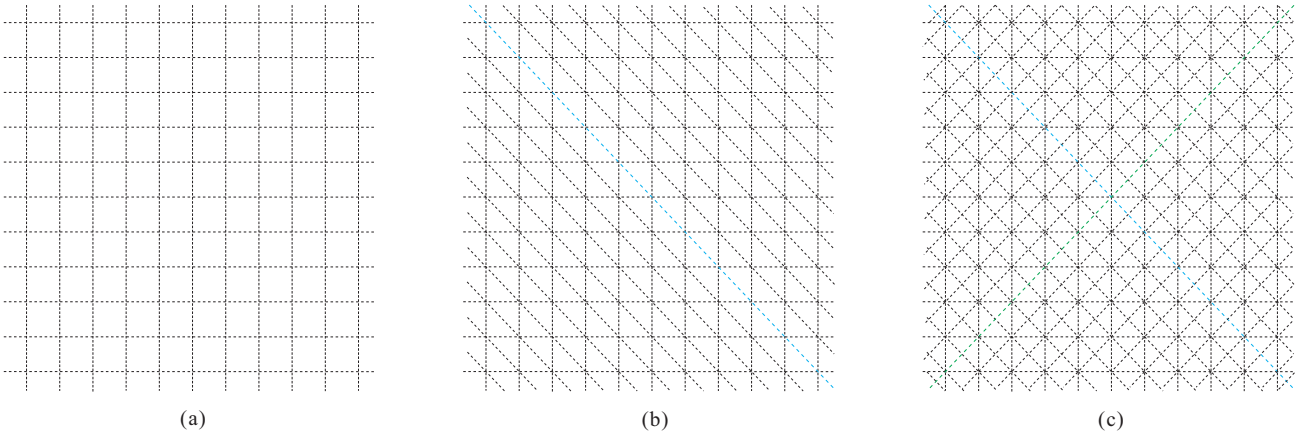

Fig. 1: A fragment of infinite graph (a) G^∞, (b) T^∞, and (c) S^∞.

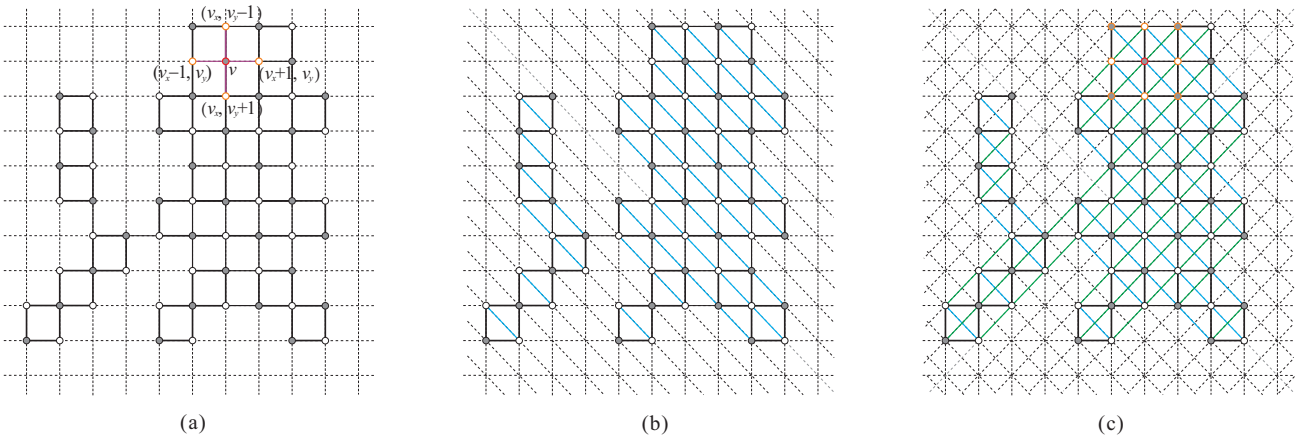

Fig. 2: (a) A grid graph, (b) a triangular grid graph, and (c) a supergrid graph, where circles represent the vertices and solid lines indicate the edges in the graphs.

(v_x, v_y+1), (v_x-1, v_y-1), and (v_x+1, v_y+1). For example, Fig. 2(b) shows a triangular grid graph. Thus, triangular grid graphs contain grid graphs as subgraphs. Note that triangular grid graphs defined above are isomorphic to the original triangular grid graphs studied in the literature [12] but these graphs are different when considered as geometric graphs. By the same construction of triangular grid graphs from grid graphs, we have proposed a new class of graphs, namely *supergrid graphs*, in [18]. The *two-dimensional supergrid* S^∞ is an infinite graph obtained from T^∞ by adding all edges on the lines traced from up-right to down-left. A *supergrid graph* is a finite, vertex-induced subgraph of S^∞. The possible adjacent vertices of a vertex $v = (v_x, v_y)$ in a supergrid graph include (v_x, v_y-1), (v_x-1, v_y), (v_x+1, v_y), (v_x, v_y+1), (v_x-1, v_y-1), (v_x+1, v_y+1), (v_x+1, v_y-1), and (v_x-1, v_y+1). Then, supergrid graphs contain grid graphs and triangular grid graphs as subgraphs. For example, Fig. 1(c) depicts a fragment of graph S^∞ and Fig. 2(c) shows a supergrid graph. Notice that grid and triangular grid graphs are not subclasses of supergrid graphs, and the converse is also true: these classes of graphs have common elements (points) but in general they are distinct since the edge sets of these graphs are different. Obviously, all grid graphs are bipartite [20] but triangular grid graphs and supergrid graphs are not bipartite. The Hamiltonian cycle problem for grid graphs and triangular grid graphs were known to be NP-complete [12, 20]. Recently, we have shown that the Hamiltonian cycle problem on supergrid graphs is also NP-complete [18].

The Hamiltonian cycle problem on supergrid graphs can be applied to control the stitching trace of a computerized sewing machine as follows [18]. Consider a computerized sewing machine given an image. The computerized sewing software is used to compute the sewing traces of a computerized sewing machine. A computerized sewing software may include two parts. The first part is to do image processing for the input image, eg., reduce order of colors and image thinning. It then produces some sets of lattices in which every set of lattices represents a color in the input image for sewing. The second part is given by a set of lattices and then computes a cycle (path) to visit the lattices of the set such that each lattice is visited exactly once. Finally, the software transmits the stitching trace of the computed cycle

(path) to the computerized sewing machine, and the machine then performs the sewing work along the trace on the object, e.g. clothes. For example, given an image in Fig. 3(a), the software first analyzes the image and then produces ten colors of regions in which each region is filled with the same color and may be formed by some blocks, as shown in Fig. 3(b). It then produces ten sets of lattices in which every set of lattices represents a region, where each region is filled by a sewing trace with the same color and it may be partitioned into many non-contiguous blocks. Fig. 3(c) shows a set of lattices for one region of color, and the software then computes a sewing trace for the set of lattices, as depicted in Fig. 3(d). Since each stitch position of a sewing machine can be moved to its eight neighbor positions (left, right, up, down, up-left, up-right, down-left, and down-right), one set of adjacent lattices forms a supergrid graph which may be disconnected. Note that each lattice will be represented by a vertex of a supergrid graph, each region may be separated by many blocks in which each block represented a connected supergrid graph. The desired sewing trace of each set of adjacent lattices is the Hamiltonian cycle (path) of the corresponding connected supergrid graph when it is Hamiltonian. Note that if the corresponding supergrid graph is not Hamiltonian, then the sewing trace contains more than one paths and these paths must be concatenated by jump lines. After computing the sewing traces of all regions of colors, the software then transmits the computed stitching trace to the computerized sewing machine. Fig. 3(e) depicts the final sewing result for the image in Fig. 3(a). In addition, the structure of supergrid graphs can be used to design the topology of networks, and the network diameter of the proposed supergrid graphs is smaller than that of grid graphs.

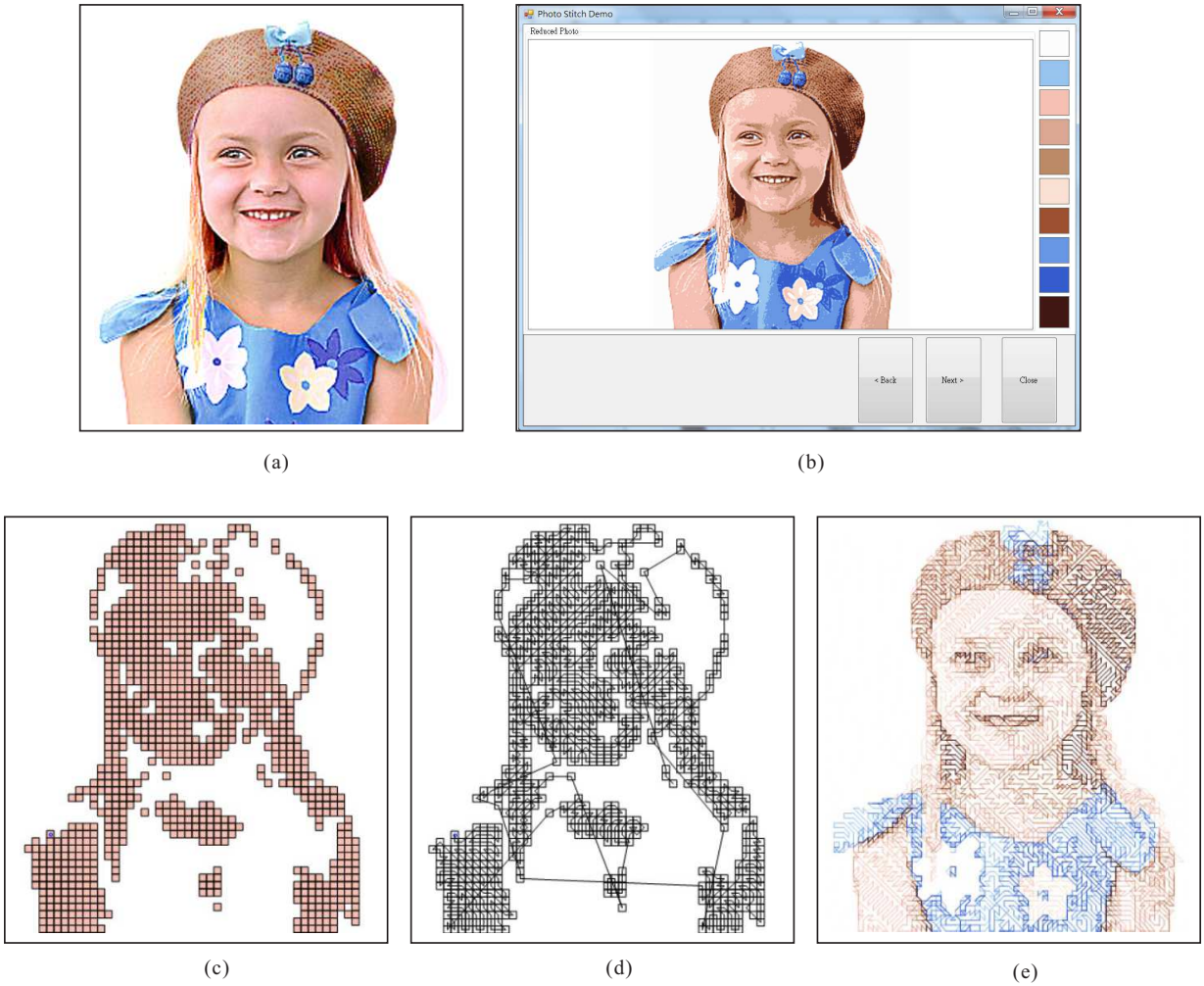

Fig. 3: (a) An input image for the computerized sewing software, (b) ten colors of regions produced by image processing, (c) a set of lattices for one region of color, (d) a possible sewing trace for the set of lattices in (c), and (e) an overview after computing sewing traces and cutting all jump lines of all regions of colors.

In this paper, we will study the Hamiltonian property of a subclass of supergrid graphs, called *linear-convex supergrid graphs*. A supergrid graph G is *linearly convex* if, for every line l which contains an edge of S^{∞}, the intersection of l and G is either a line segment (a path in G), or a point (a vertex in G), or empty. Linear-convex

triangular grid graphs are defined similarly. In general, a linear-convex supergrid graph is always a linear-convex triangular grid graph with the same vertex set, but the reverse is not true. For example, a linear-convex triangular grid graph T is shown in Fig. 4(a), but its corresponding supergrid graph with vertex set $V(T)$ is not linear convex, as shown in Fig. 4(b). In [12, 31], the authors showed that any 2-connected, linear-convex triangular grid graph with the exception of the Star of David graph always contains a Hamiltonian cycle. However, the result can not be applied to 2-connected, linear-convex supergrid graphs. In this paper, we first show that any 2-connected, linear-convex supergrid graph is locally connected. We then prove that any 2-connected, linear-convex supergrid graph contains a Hamiltonian cycle.

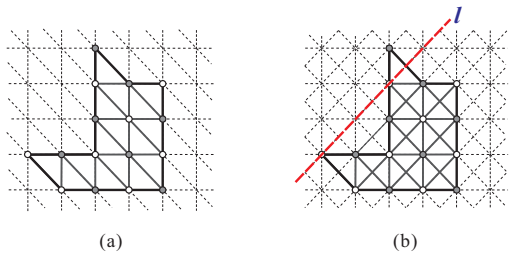

Fig. 4: (a) A linear-convex triangular grid graph T, and (b) a supergrid graph S with vertex set $V(T)$ which is not linearly convex, where the intersection of line l and graph S contains two isolated vertices.

Related works of investigation are summarized as follows. Itai et al. [20] showed that the Hamiltonian cycle and path problems for grid graphs are NP-complete. They also gave the necessary and sufficient conditions for a rectangular grid graph having a Hamiltonian path between two given vertices. Zamfirescu et al. [34] gave the sufficient conditions for a grid graph having a Hamiltonian cycle, and proved that all grid graphs of positive width have Hamiltonian line graphs. Later, Chen et al. [6] improved the Hamiltonian path algorithm of [20] on rectangular grid graphs and presented a parallel algorithm for the Hamiltonian path problem with two given endpoints in rectangular grid graph (mesh). Also there is a polynomial-time algorithm for finding Hamiltonian cycles in solid grid graphs [25]. In [32], Salman introduced alphabet grid graphs and determined classes of alphabet grid graphs which contain Hamiltonian cycles. Recently, Keshavarz-Kohjerdi and Bagheri [22] gave the necessary and sufficient conditions for the existence of Hamiltonian paths in alphabet grid graphs, and presented linear-time algorithms for finding Hamiltonian paths with two given endpoints in these graphs. Recently, Keshavarz-Kohjerdi et al. [23] presented a linear-time algorithm for computing the longest path between any two given vertices in rectangular grid graphs. Reay and Zamfirescu [31] proved that all 2-connected, linear-convex triangular grid graphs except one special case contain Hamiltonian cycles. The Hamiltonian cycle (path) for triangular grid graphs has been shown to be NP-complete [12]. They also proved that all connected, locally connected triangular grid graphs (with one exception as in [31]) contain Hamiltonian cycles. The Hamiltonian cycle problem on hexagonal grid graphs has been shown to NP-complete [19]. Recently, we have proved the Hamiltonian cycle (path) problem for supergrid graphs to be NP-complete [18]. For more works of investigation on grid and triangular grid graphs, we refer readers to [5, 8, 13, 17, 26, 27, 28, 35].

The rest of the paper is organized as follows. In Section 2, we give some notations and observations. Section 3 shows that any 2-connected, linear-convex supergrid graph is locally connected. In Section 4, we show that any 2-connected, linear-convex supergrid graph contains a Hamiltonian cycle. Finally, we make some concluding remarks in Section 5.

2 Preliminaries

In this section, we will introduce some technologies and symbols. Some useful observations are also given. For graph-theoretic terminology not defined in this paper, the reader is referred to [4]. Let $G = (V, E)$ be a graph with vertex set $V(G)$ and edge set $E(G)$. Let S be a subset of vertices in G, and let u, v be two vertices in G. We write $G[S]$ for the subgraph of G *induced* by S, $G - S$ for the subgraph $G[V - S]$, i.e., the subgraph induced by $V - S$. In general, we write $G - v$ instead of $G - \{v\}$. If (u, v) is an edge in G, we say that u is *adjacent* to v and u, v are *incident* to edge (u, v). The notation $u \sim v$ (resp., $u \nsim v$) means that vertices u and v are adjacent (resp., non-adjacent). A *neighbor* of v in G is any vertex that is adjacent to v. We use $N_G(v)$ to denote the set of neighbors of v in G and remove the subscript 'G' of $N_G(v)$ from the notation if it has no ambiguity. The degree of v is the number of vertices adjacent to vertex v, and denoted by $deg(v) = |N(v)|$. The *distance* between u and v is the length of the shortest path between those two vertices.

A path P of length $|P| - 1$ in G, denoted by $v_1 \to v_2 \to \cdots \to v_{|P|-1} \to v_{|P|}$, is a sequence $(v_1, v_2, \cdots, v_{|P|-1}, v_{|P|})$

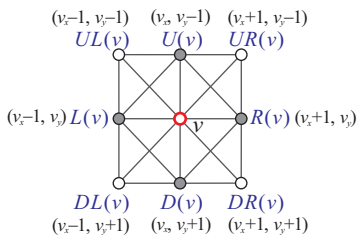

Fig. 5: The possible neighbors of vertex $v = (v_x, v_y)$ in a supergrid graph.

of vertices such that $(v_i, v_{i+1}) \in E(G)$ and $v_i \neq v_{i+1}$ for $1 \leqslant i < |P|$. The first and last vertices visited by P are called the *path-start* and *path-end* of P, denoted by $start(P)$ and $end(P)$, respectively. We will use $v_i \in P$ to denote "P visits v_i". A path from vertex v_1 to another vertex v_k is denoted by (v_1, v_k)-path. In addition, we use P to refer to the set of vertices visited by path P if it is understood without ambiguity. On the other hand, a path is called the *reversed path*, denoted by $\text{rev}(P)$, of path P if it visits the vertices of P from $end(P)$ to $start(P)$ sequentially; that is, the reversed path $\text{rev}(P)$ of $P = v_1 \to v_2 \to \cdots \to v_{|P|-1} \to v_{|P|}$ is $v_{|P|} \to v_{|P|-1} \to \cdots \to v_2 \to v_1$. A cycle is a path C with $|V(C)| \geqslant 3$ and $start(C) \sim end(C)$. As usually, we use P_k and C_k to denote the path and cycle of k vertices, respectively.

A cycle C in a graph G is *extendable* if there exists a cycle C' in G (called the *extension* of C) such that $V(C) \subset V(C')$ and $|V(C')| = |V(C)| + 1$. If such a cycle C' exists, we say that C can be extended to C'. A graph G is called *cycle extendable* if G has at least one cycle and if every non-hamiltonian cycle in G is extendable. The cycle extendable graphs form a subclass of Hamiltonian graphs [16]. Thus, every cycle extendable graph is Hamiltonian.

We next give some observations on the relations among cycle, path, and vertex in the following. Let C be a cycle of a graph and let vertex $x \notin C$. If there exists an edge u, v in C such that $u \sim x$ and $v \sim x$, then $C \to x$ is a cycle of the graph, where $start(C), end(C) \in \{u, v\}$. Thus the following proposition holds true.

Proposition 2.1. *Let C be a cycle of a graph G and let x be a vertex in $G - V(C)$. If there exists an edge (u, v) in C such that $u \sim x$ and $v \sim x$, then C and x can be merged into a cycle of G.*

The above observation can be extended to a path P as the following proposition.

Proposition 2.2. *Let C and P be a cycle and a path, respectively, of a graph G such that $V(C) \cap V(P) = \emptyset$. If there exists an edge (u, v) in C such that $u \sim start(P)$ and $v \sim end(P)$, then C and P can be concatenated into a cycle of G.*

Let C_1 and C_2 be two vertex-disjoint cycles of a graph G. If there exist two edges $(u_1, v_1) \in C_1$ and $(u_2, v_2) \in C_2$ such that $u_1 \sim u_2$ and $v_1 \sim v_2$, then $C_1 \to C_2$ is a cycle of G, where $end(C_1) = v_1$ and $start(C_2) = v_2$. Thus we have the following proposition.

Proposition 2.3. *Let C_1 and C_2 be two vertex-disjoint cycles of a graph G. If there exist two edges $(u_1, v_1) \in C_1$ and $(u_2, v_2) \in C_2$ such that $u_1 \sim u_2$ and $v_1 \sim v_2$, then C_1 and C_2 can be concatenated into a cycle of G.*

Let C_1 and C_2 be two cycles of a graph G such that $V(C_1) \cap V(C_2) = \{v\}$. If there exist two edges $(u, v) \in C_1$ and $(w, v) \in C_2$ such that $u \sim w$, then $C_1 \to C_2$ forms a cycle of G, where $end(C_1) = u$ and $start(C_2) = w$. Hence, the following observation is true.

Proposition 2.4. *Let C_1 and C_2 be two cycles of a graph G such that $V(C_1) \cap V(C_2) = \{v\}$. If there exist two edges $(u, v) \in C_1$ and $(w, v) \in C_2$ such that $u \sim w$, then C_1 and C_2 can be concatenated into a cycle of G.*

Let S^∞ be the infinite graph whose vertex set consists of all points of the plane with integer coordinates and in which two vertices are adjacent if and only if the difference of their x or y coordinate is not larger than 1. A *supergrid graph* is a finite, vertex-induced subgraph of S^∞. For a vertex v in a supergrid graph, let v_x and v_y denote x and y coordinates of v, respectively. We color vertex v to be *white* if $v_x + v_y \equiv 0 \pmod 2$; otherwise, v is colored to be *black*. Then there are eight possible neighbors of vertex v including four white vertices and four black vertices. For simplicity, we denote the possible neighbors of $v = (v_x, v_y)$ as $UL(v) = (v_x - 1, v_y - 1)$ (up-left), $U(v) = (v_x, v_y - 1)$ (up), $UR(v) = (v_x + 1, v_y - 1)$ (up-right), $L(v) = (v_x - 1, v_y)$ (left), $R(v) = (v_x + 1, v_y)$ (right), $DL(v) = (v_x - 1, v_y + 1)$ (down-left), $D(v) = (v_x, v_y + 1)$ (down), and $DR(v) = (v_x + 1, v_y + 1)$ (down-right). Fig. 5 depicts the possible neighbors of vertex v in a supergrid graph. For example, $u = UL(v)$ means that vertex u is the up-left neighbor of vertex v.

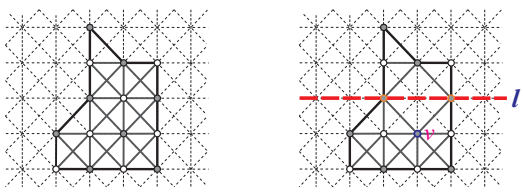

Fig. 6: (a) A linear-convex supergrid graph, and (b) a supergrid graph which is not linearly convex, where solid lines indicate edges of graphs and the bold dashed line l indicates that the intersection of l and the graph in (b) contains two isolated vertices.

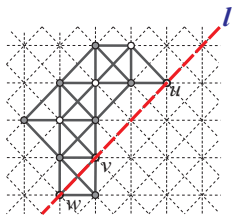

Fig. 7: A locally connected, but not linear-convex supergrid graph, where solid lines indicate edges of graphs and the bold dashed line l contains edges of S^{∞}.

A supergrid graph G is *linearly convex* if, for every line l which contains an edge of S^{∞}, the intersection of l and G is either a line segment (a path in G), or a point (a vertex in G), or empty. For example, Fig. 6(a) is a linear-convex supergrid graph but Fig. 6(b) is not a linear-convex supergrid graph since there exists at least one line l in S^{∞} such that the intersection of l and G includes two isolated vertices.

Let v be a vertex in a linear-convex supergrid graph G. We observe that if both $UL(v)$ and $UR(v)$ are vertices in G, then $U(v)$ is also a vertex in G; otherwise, we can find a parallelism line l passing through $UL(v)$, $UR(v)$ but not passing through $U(v)$, and the intersection of l and G contains at least two paths of G. For example, Fig. 6(b) depicts such a situation. Thus, we have the following proposition.

Proposition 2.5. *Let v be a vertex of a linear-convex supergrid graph G. If $UL(v)$ and $UR(v)$ (resp., $UL(v)$ and $DL(v)$, $UR(v)$ and $DR(v)$, $DL(v)$ and $DR(v)$) are in G, then $U(v)$ (resp., $L(v)$, $R(v)$,$D(v)$) is in G.*

3 Local connectivity of linear-convex supergrid graphs

In this section, we will establish an interrelation between 2-connected, linear-convex supergrid graphs and locally connected supergrid graphs. Recall that a graph G is 2-connected if there are two vertex-disjoint paths between every pair of vertices in G, and G is locally connected if for every vertex u in G, the induced subgraph $G[N(u)]$ of G is connected. A locally connected supergrid graph is not necessary to be linearly convex. For example, Fig. 7 shows a locally connected supergrid graph, which is not linearly convex: the intersection of the graph and the bold dashed line l is the union of a point (the vertex u of the graph) and a line segment (the edge (v, w) of the graph). In the following theorem, we will prove that any 2-connected, linear-convex supergrid graph is locally connected.

Theorem 3.1. *Let G be a 2-connected, linear-convex supergrid graph. Then, G is locally connected.*

Proof. We prove this theorem by contradiction. Assume by contradiction that G contains a vertex u such that u is not locally connected. Then, $G[N(u)]$ is not connected. The 2-connectedness of G implies that $deg(u) \geqslant 2$. On the other hand, if $deg(u) = 7$ or 8, then $G[N(u)]$ is connected and contains a path P_7 or C_8 as subgraph. Thus, $deg(u) \leqslant 6$. Then, $2 \leqslant deg(u) \leqslant 6$. Consider the following five possible cases for the degree of u.

Case 1: $deg(u) = 2$. Let $N(u) = \{v, w\}$. Then, $v \nsim w$. By symmetry, we need only consider the subcases, as shown in Fig. 8. Consider the subcase in Fig. 8(a). Then, $v = UL(u)$ and $w = UR(u)$. By Proposition 2.5, $U(u)$ is in G and it contradicts that $deg(u) = 2$. On the other hand, consider the subcase in Fig. 8(b). Then, $v = UL(u)$ and $w = R(u)$. Since G is 2-connected, there exists a (v, w)-path P in G with internal vertices different from u. Let l be a line which contains the edge $(U(u), u)$ of S^{∞}. Then, the intersection of l and G contains vertex u as an isolated vertex (since $U(u)$ and $D(u)$ are not in G) and at least one vertex of P. This contradicts that G is linearly convex.

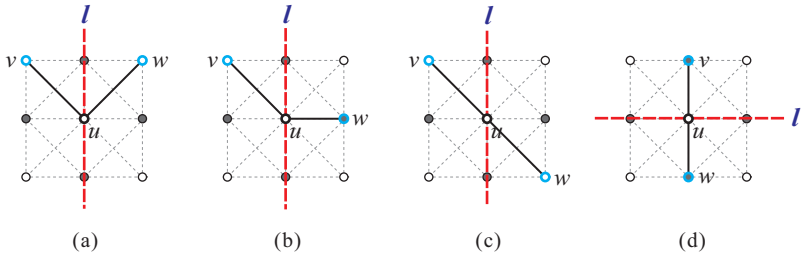

Fig. 8: The possible subcases for $deg(u) = 2$ in the proof of Theorem 3.1, where the lines l of S^∞ used to obtain a contradiction are drawn by bold dashed lines.

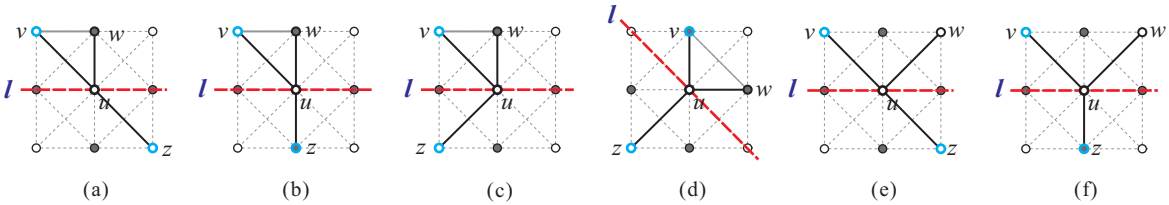

Fig. 9: The possible subcases for $deg(u) = 3$ in the proof of Theorem 3.1, where the lines l of S^∞ used to obtain a contradiction are drawn by bold dashed lines.

The other subcases can be proved by the same arguments. Fig. 8(c)–(d) also depicts the lines l of S^∞ used to obtain a contradiction.

Case 2: $deg(u) = 3$. Let $N(u) = \{v, w, z\}$. In this case, the possible related locations among u, v, w, z are depicted in Fig. 9. Consider the subcase of Fig. 9(a). Then, $v = UL(u)$, $w = U(u)$, and $z = DR(u)$. Since G is 2-connected, there exists a (v, z)-path P in G with internal vertices different from u. Let l be a line which contains the edge $(L(u), u)$ of S^∞. Then, the intersection of l and G contains vertex u as an isolated vertex (since $L(u)$ and $R(u)$ are not in G) and at least one vertex of P. This contradicts that G is linearly convex. By the same arguments, we can find a line l of S^∞ to get a contradiction for the other cases. Fig. 9(b)–(f) also depict these lines.

Case 3: $deg(u) = 4$. Let $N(u) = \{v, w, z, x\}$. By symmetry, the possible related locations among u, v, w, z, x are shown in Fig. 10. For the subcases of Fig. 10(a)–(d), we can obtain a contradiction by similar arguments in proving Case 1, where there exists a (v, x)-path in G with internal vertices different from u. Consider the subcase of Fig. 10(e). Then, $v = UL(u)$, $w = U(u)$, $z = R(u)$, and $x = DL(u)$. Since G is 2-connected, there exists a (v, x)-path P in G with internal vertices different from u. Let l_1 be a line which contains the edge (u, z) of S^∞, and let l_2 be a line which contains the edge (v, u) of S^∞. Clearly, the intersection of l_1 and G contains the edge (u, z) but does not contain $L(u)$, and the intersection of l_2 and G contains the edge (v, u) but does not contain $DR(u)$. Let l_1' and l_2' be two part rays of l_1 and l_2, respectively, such that l_1' starts from u and passes $L(u)$, and l_2' starts from u and passes $DR(u)$. Then, the intersection of $l_1' \cup l_2'$ and G contains at least one vertex of P. This contradicts that G is linearly convex. By the same arguments, we can arrive at a contradiction for the other subcases of Fig. 10(f)–(h) which also indicate lines l_1 and l_2 in these subcases.

Case 4: $deg(u) = 5$. Let $N(u) = \{x_1, x_2, x_3, x_4, x_5\}$. By symmetry, the possible related locations among u, x_1, x_2, x_3, x_4, x_5 are shown in Fig. 11(a)–(d). The proofs of subcases in Fig. 11(a)–(b) are similar to the proof of Case 1, and the proofs of subcases in Fig. 11(c)–(d) are similar to the proof of Case 3 in Fig. 10(e), where there exists a (x_1, x_5)-path in G with internal vertices different from u.

Case 5: $deg(u) = 6$. Let $N(u) = \{x_1, x_2, x_3, x_4, x_5, x_6\}$. By symmetry, the possible related locations among $u, x_1, x_2, x_3, x_4, x_5, x_6$ are shown in Fig. 11(e)–(f). The proof of subcase in Fig. 11(e) is similar to the proof of Case 1. And the proof of subcase in Fig. 11(f) is similar to the proof of Case 3 in Fig. 10(e). Note that there exists a (x_1, x_6)-path in G with internal vertices different from u.

It follows from the above cases that a contradiction occurs, and, hence, every vertex of a 2-connected, linear-convex supergrid graph is locally connected. Thus, a 2-connected, linear-convex supergrid graphs is locally connected. This completes the proof. □

Let G be a 2-connected, linear-convex supergrid graph and let u be a vertex in G. Since G is 2-connected, $deg(u) \geqslant 2$. By Theorem 3.1, G is locally connected. Thus, there exist two vertices v, w of $N(u)$ such that (v, w) is an edge of G. Then, $u \to v \to w$ is a cycle of G. Thus, we have the following corollary.

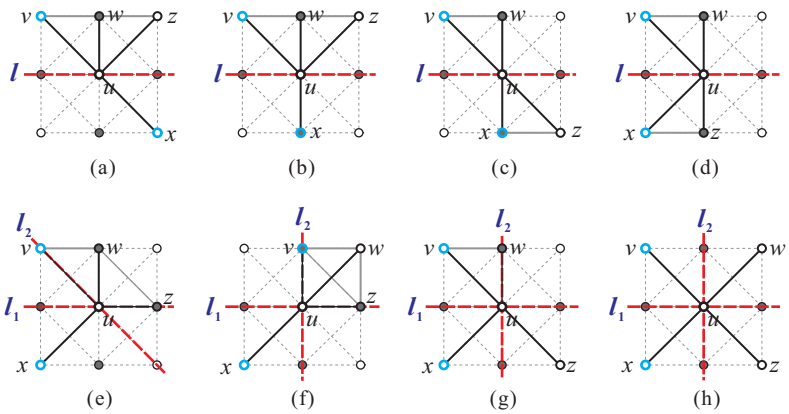

Fig. 10: The possible subcases for $deg(u) = 4$ in the proof of Theorem 3.1, where the lines l of S^{∞} used to obtain a contradiction are drawn by bold dashed lines.

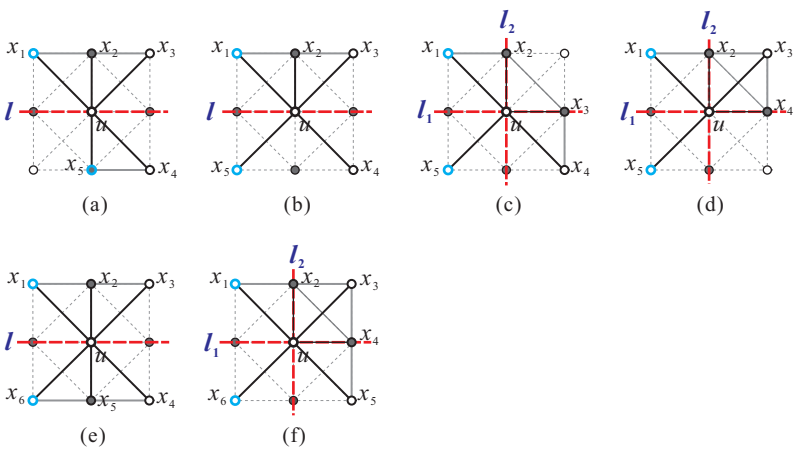

Fig. 11: The possible subcases for $deg(u) = 5$ and $deg(u) = 6$ in the proof of Theorem 3.1, where (a)–(d) are subcases of $deg(u) = 5$ and (e)–(f) are subcases of $deg(u) = 6$.

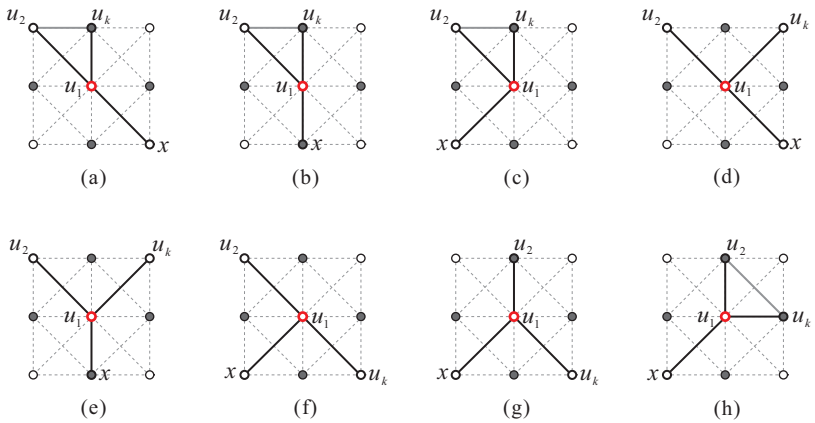

Fig. 12: The possible relative locations among u_1, u_2, u_k, x when $x \sim u_1$, $x \nsim u_2$, and $x \nsim u_k$.

Corollary 3.2. *If G is a 2-connected, linear-convex supergrid graph, then G contains at least one cycle.*

4 The Hamiltonian cycle problem on linear-convex supergrid graphs

In this section, we consider connected graphs on $n \geqslant 3$ vertices. We will prove that every 2-connected, linear-convex supergrid graph is cycle extendable. The result implies that every 2-connected, linear-convex supergrid graph contains a Hamiltonian cycle. The main result is shown as follows.

Theorem 4.1. *Let G be a 2-connected, linear-convex supergrid graph. Then, G is cycle extendable.*

Proof. By Corollary 3.2, G contains at least one cycle. Since G is 2-connected, the degree of every vertex in G is at least 2. We will prove this theorem by contradiction. Assume by contradiction that G is not cycle extendable. Then, there exists a non-extendable, non-Hamiltonian cycle C of G. Let $C = u_1 \to u_2 \to u_3 \to \cdots \to u_{k-1} \to u_k$ with $k < |V(G)|$, where $u_1 \sim u_k$. Since G is connected, there exists a vertex x not in C which is adjacent to one vertex lying on C. Without loss of generality, let u_1 be such a vertex on C with $u_1 \sim x$. Then, $3 \leqslant deg(u_1) \leqslant 8$. By Proposition 2.1, if $x \sim u_2$ or $x \sim u_k$ then C can be extended to cover x, a contradiction. Thus, $x \nsim u_2$ and $x \nsim u_k$. Depending on whether $u_2 \sim u_k$ and the symmetry, we need only consider the cases, as shown in Fig. 12, for the related positions among u_1, u_2, u_k, x.

Let $Z = \{L(u_1), R(u_1)\} - \{u_2, u_k\}$. We can select set Z to satisfy that $Z \cap V(G) \neq \emptyset$ as follows. Consider the cases of Fig. 12(a)–(g). Suppose that $Z \cap V(G) = \emptyset$. Since G is 2-connected, there exists a (u_2, x)-path P in G with internal vertices different from u_1. Let l be a line which contains edge $(L(u_1), u_1)$ of S^∞. Then, the intersection of l and G contains vertex u_1 as an isolated vertex and at least one vertex of P. It contradicts that G is linearly convex. Thus, $Z \cap V(G) \neq \emptyset$. On the other hand, consider the case of Fig. 12(h). By similar arguments in proving Case 3 (Fig. 10(f)) of Theorem 3.1, we can verify that $\{L(u_1), D(u_1)\} \cap V(G) \neq \emptyset$. By symmetry, we can let $L(u_1) \in V(G)$. Thus, we can select Z with $Z \cap V(G) \neq \emptyset$. We then select a vertex z of Z to satisfy the following condition:

(C1) if one of $Z \cap V(G)$ is adjacent to vertex x, then let z be the vertex with $z \sim x$; otherwise, $z \in Z \cap V(G)$ with $z \nsim x$.

The above condition implies that if $z \nsim x$ then none of $Z \cap V(G)$ is adjacent to x. By inspecting all cases of Fig. 12, z is adjacent to at least one of u_2 and u_k. Since $(u_1, u_2) \in C$, $(u_1, u_k) \in C$, $z \sim u_1$, and ($z \sim u_2$ or $z \sim u_k$), by Proposition 2.1 $z \in C$. If $z \sim u_k$ and $z \nsim u_2$, then we can exchange the positions of u_2 and u_k because of the symmetric structure of a cycle. Thus, we may assume that $z \sim u_2$ below. We proceed via the following two statements toward a final contradiction.

1. If $z \sim x$, then C can be extended to cover x, i.e., C and x can be merged into a cycle.
2. If $z \nsim x$, then C can be extended to cover x.

Summarizing the above statements, we conclude that C is cycle extendable. It contradicts that C is a non-extendable, non-Hamiltonian cycle of G. This completes the proof of the theorem. □

The proofs of the above two statements are given below as Claims 1–2. We will prove these two claims by constructing a cycle C' extended from C to cover vertex x.

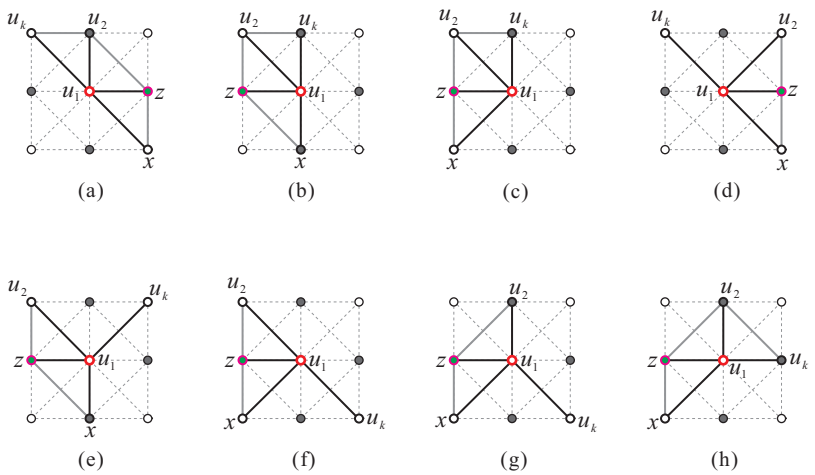

Fig. 13: The possible relative locations among u_1, u_2, u_k, x, and z under that $z \sim x$ and $z \sim u_2$, where $z \in \{L(u_1), R(u_1)\} - \{u_2, u_k\}$.

Claim 1. If $z \sim x$, then C can be extended to cover x.

Proof. By inspecting the cases in Fig. 12, the possible locations among u_1, u_2, u_k, x, and z under $z \sim x$ are shown in Fig. 13. Note that $z \sim u_2$, $z \sim x$, and we can exchange the locations of u_2 and u_k by symmetry. Since $(u_1, u_2) \in C$, $z \sim u_1$, and $z \sim u_2$, we get $z \in C$ by Proposition 2.1. Let $z = u_j$. Then, $2 < j < k$. If $x \sim u_{j-1}$ or $x \sim u_{j+1}$, then by Proposition 2.1, C can be extended to cover x since $x \sim z$. In the following, assume that $x \nsim u_{j-1}$ and $x \nsim u_{j+1}$. Consider that $u_{j-1} \sim u_{j+1}$. Let $P_1 = u_2 \to u_3 \to \cdots \to u_{j-1}$ and let $P_2 = u_{j+1} \to u_{j+2} \to \cdots \to u_k$. Then, $u_1 \to x \to u_j(= z) \to P_1 \to P_2$ is a cycle of $G[V(C) \cup \{x\}]$, a contradiction. In the following, assume that $u_{j-1} \nsim u_{j+1}$. Then, the following condition is satisfied:

(C2) $z(= u_j) \sim u_2$, $z \sim x$, $x \nsim u_{j-1}$, $x \nsim u_{j+1}$, and $u_{j-1} \nsim u_{j+1}$.

We first consider the case of $j = 3$. Then, $u_2 = u_{j-1}$ and hence $(u_2, u_3 = z)$ is an edge in C. Suppose that $u_2 \sim u_k$. Let $C_1 = u_1 \to x \to u_3(= z)$ and let $C_2 = u_2 \to u_3 \to \cdots \to u_{k-1} \to u_k$. Then, $V(C_1) \cap V(C_2) = \{u_3 = z\}$. Since $u_1 \sim u_2$, C_1 and C_2 can be merged into a cycle by Proposition 2.4. On the other hand, suppose that $u_2 \nsim u_k$. By Proposition 2.1, $x \nsim u_4$ since $x \sim u_3 = z$ and $(u_3, u_4) \in C$. Then, $u_4 \in N(z)$, $u_2 \nsim u_4$ ($u_{j-1} \nsim u_{j+1}$), $u_2 \nsim u_k$, and $x \nsim u_4$. That is, the possible cases must satisfy that $N(z) - (N(x) \cup N(u_2)) \neq \emptyset$. By examining every case in Fig. 13, the possible cases (Fig. 13(e) and (g)) are depicted in Fig. 14 under that condition (C2) is satisfied, $u_3 = z$, and $u_2 \nsim u_k$. Consider the case of Fig. 14(a). Then, $N(z) - (N(x) \cup N(u_2)) = \{DL(z)\}$. Thus, $u_4 = DL(z)$. Since $DL(z)$ and $DR(z)(= x)$ are in G, we obtain that $D(z)$ is in G by Proposition 2.5. Since $D(z) \sim z(= u_3)$, $D(z) \sim DL(z) = u_4$, and $(z, DL(z)) \in C$, we get that $D(z) \in C$ by Proposition 2.1. Let $y = D(z) = u_t$. Then, $4 < t \leqslant k - 1$. Clearly, $x \sim z$, $y \sim z$, and $y \sim x$. If $u_{t-1} \sim u_{t+1}$, then $u_1 \to x \to y(= u_t) \to z(= u_3) \to u_4 \to u_5 \to \cdots \to u_{t-1} \to u_{t+1} \to u_{t+2} \to \cdots \to u_{k-1} \to u_k$ forms a cycle containing $V(C)$ and x. Suppose that $u_{t-1} \nsim u_{t+1}$. If $u_{t-1} \sim x$ or $u_{t+1} \sim x$, then x can be merged into C by Proposition 2.1. Thus, $u_{t-1} \nsim x$ and $u_{t+1} \nsim x$. Then, $\{u_{t-1}, u_{t+1}\} = \{UL(y), DL(y)\}$. Let $u_{t-1} = UL(y)$ and $u_{t+1} = DL(y)$. Then, $C = u_1 \to u_2 \to u_3(= z) \to u_4(= DL(z)) \to P_1 \to u_{t-1} \to y(= u_t) \to u_{t+1} \to P_2$, where $end(P_2) = u_k$. Let $C' = u_1 \to u_2 \to u_{t-1} \to \mathrm{rev}(P_1) \to u_4 \to z \to x \to y \to u_{t+1} \to P_2$. Then, C' is a cycle that contains $V(C)$ and x. The construction of such a cycle C' is depicted in Fig. 15(a). When $u_{t-1} = DL(y)$ and $u_{t+1} = UL(y)$, the extended cycle from C and x is constructed, as shown in Fig. 15(b). By the similar construction, we can construct an extended cycle C' for the case of Fig. 14(b), as shown in Fig. 15(c)–(d).

In the following, we will consider the case of $j > 3$. Then, $u_2 \neq u_{j-1}$. Note that $z = u_j$. By condition (C2), $x \nsim u_{j-1}$, $x \nsim u_{j+1}$, and $u_{j-1} \nsim u_{j+1}$. By inspecting all cases in Fig. 13, the cases of Fig. 13(a)(c)(g)(h) do not satisfy condition (C2). Thus, the possible cases under condition (C2) and $j > 3$ are depicted in Fig. 16. Consider the cases of Fig. 16(b) and (d). We can see that $\{u_{j-1}, u_{j+1}\} = \{UL(z), UR(z)\}$. Let $C = u_1 \to u_2 \to P_1 \to z \to P_2 \to u_k$, where $end(P_1) = u_{j-1}$ and $start(P_2) = u_{j+1}$. Let $C' = u_1 \to x \to z \to \mathrm{rev}(P_1) \to u_2 \to P_2 \to u_k$. Then, C' is a Hamiltonian cycle of $G[V(C) \cup \{x\}]$ and is extended from C by adding x. Now, consider the case of Fig. 16(a). We can see that $\{u_{j-1}, u_{j+1}\} = \{UL(z), DL(z)\}$. Since $UL(z)$, $DL(z)$, and $DR(z)(= x)$ are in G, both $L(z)$ and $D(z)$ are in G by Proposition 2.5. Let $y = D(z)$. Then, $y \sim x$. Since $y \sim z$, $y \sim DL(z)$, and $(z, DL(z)) \in C$, we get that $y \in C$ by Proposition 2.1. Let $y = u_t$. If $x \sim u_{t-1}$ or $x \sim u_{t+1}$, then a Hamiltonian cycle of $G[V(C) \cup \{x\}]$ can be constructed

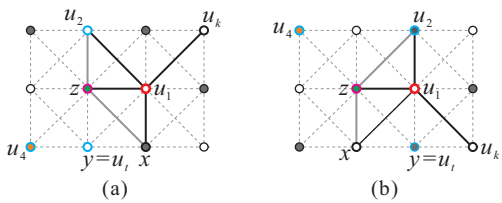

Fig. 14: The possible cases (Fig. 13(e) and (g)) under that condition (C2) is satisfied, $z = u_3$, and $u_2 \nsim u_k$.

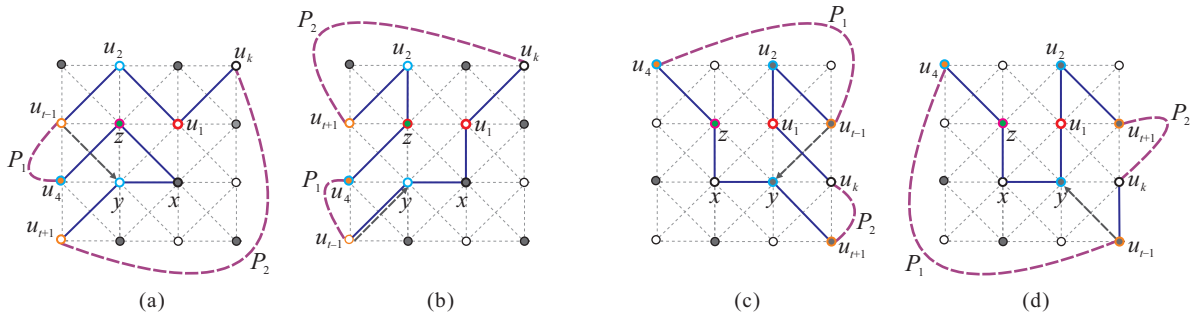

Fig. 15: (a)–(b) The constructions of extended cycles C' for the case of Fig. 14(a); and (c)–(d) the constructions of extended cycles C' for the case of Fig. 14(b), where solid edges indicate the edges in the cycles, bold dashed lines represent the subpaths P_1 and P_2 of cycle C, and dashed arrow line indicates edge $(u_{t-1}, u_t(= y))$ in C.

by Proposition 2.1. Thus, assume that $x \nsim u_{t-1}$ and $x \nsim u_{t+1}$ below. Then, $L(y)(= DL(z)) \in \{u_{j-1}, u_{j+1}\}$ and $u_{t-1}, u_{t+1} \in \{UL(y), L(y), DL(y)\}$. Thus, $1 \geqslant |\{u_{j-1}, u_{j+1}\} \cap \{u_{t-1}, u_{t+1}\}| \geqslant 0$. There are two cases:

Case 1: $|\{u_{j-1}, u_{j+1}\} \cap \{u_{t-1}, u_{t+1}\}| = 1$. Then, $\{u_{j-1}, u_{j+1}\} \cap \{u_{t-1}, u_{t+1}\} = \{L(y)\}$. Depending on whether y appears before z in C, we consider the following two subcases:

Case 1.1: $2 \leqslant t \leqslant j-2$. In this subcase, $y(= u_t)$ appears before $z(= u_j)$ in C. Then, $u_{t+1} = u_{j-1} = L(y) = DL(z)$. Let $C = u_1 \to u_2 \to P_1 \to y \to u_{t+1} \to z \to P_2 \to u_k$, where $end(P_1) = u_{t-1}$ and $start(P_2) = u_{j+1} = UL(z)$. Let $C' = u_1 \to x \to y \to u_{t+1} \to \text{rev}(P_1) \to u_2 \to u_k \to \text{rev}(P_2) \to z$. Then, C' is a Hamiltonian cycle of $G[V(C) \cup \{x\}]$. Fig. 17(a) (resp., Fig. 17(b)) shows the cycle C' when $u_{t-1} = UL(y)$ (resp., $u_{t-1} = DL(y)$).

Case 1.2: $j+1 \leqslant t \leqslant k-1$. In this subcase, $y(= u_t)$ appears after $z(= u_j)$ in C. Then, $u_{j+1} = u_{t-1} = L(y) = DL(z)$. By similar arguments in proving Case 1.1, we can construct an extended cycle C' from C by adding x, as shown in Fig. 17(c)–(d).

Case 2: $|\{u_{j-1}, u_{j+1}\} \cap \{u_{t-1}, u_{t+1}\}| = 0$. In this case, $\{u_{j-1}, u_{j+1}\} = \{UL(z), DL(z)\}$ and $\{u_{t-1}, u_{t+1}\} = \{UL(y), DL(y)\}$. There are two subcases:

Case 2.1: $2 \leqslant t \leqslant j-2$. Since $\{u_{j-1}, u_{j+1}\} \cap \{u_{t-1}, u_{t+1}\} = \emptyset$, $t \neq j-2$. The possible cycles of C are shown in Fig. 18. Our strategy for constructing a cycle C' combining C with x is sketched as follows. Let P_1, P_2, P_3 be three subpaths of C for connecting $u_2, u_{j-1}, u_{j+1}, u_{t-1}, u_{t+1}, u_k$. We first construct a cycle C_1 consisting of P_1, P_2, P_3, z, and y such that there exists one edge in C_1 that is incident to edge (u_1, x). By Proposition 2.2, C_1 and (u_1, x) can be concatenated into a cycle C'. Then, C' is the desired cycle constructed from C to cover x. Fig. 19(a)–(d) show the constructed cycles C' for Fig. 18(a)–(d), respectively.

Case 2.2: $j+2 \leqslant t \leqslant k-1$. Since $\{u_{j-1}, u_{j+1}\} \cap \{u_{t-1}, u_{t+1}\} = \emptyset$, $t \neq j+2$. Then, y appears after z in C. By similar arguments in proving Case 2.1, we can construct a cycle C' from $V(C)$ and x, as shown in Fig. 20.

We have proved the cases of Fig. 16(a), (b), and (d). For the case of Fig. 16(c), the possible locations of u_{j-1} and u_{j+1} are shown in Fig. 21. By similar arguments in proving the case of Fig. 16(b), the extended cycle C' from C and x for the cases of Fig. 21(a)–(g) can be constructed. Note that Fig. 21(a)–(e) also show the constructed cycles, where dashed dark lines represent subpaths of C and solid lines indicate the edges in the constructed cycles. In addition, the extended cycle C' for the case of Fig. 21(h) can be constructed by the similar construction of Fig. 16(a).

We have considered all cases under $z \sim x$ to construct a cycle C' extended from C to cover x. This completes the proof of Claim 1. □

Claim 2. If $z \nsim x$, then C can be extended to cover x.

Proof. Recall that $Z = \{L(u_1), R(u_1)\} - \{u_2, u_k\}$, $Z \cap V(G) \neq \emptyset$, and $z \in Z$. We select vertex z to satisfy condition

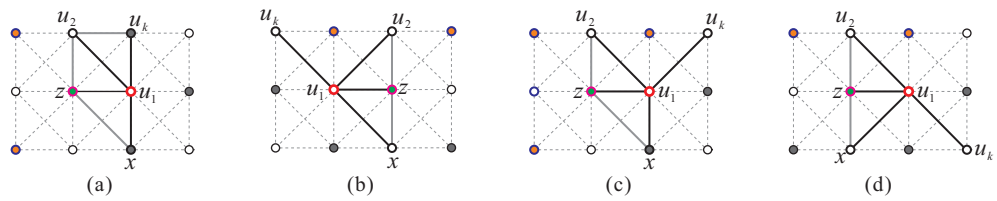

Fig. 16: The possible cases under condition (C2) and $j > 3$.

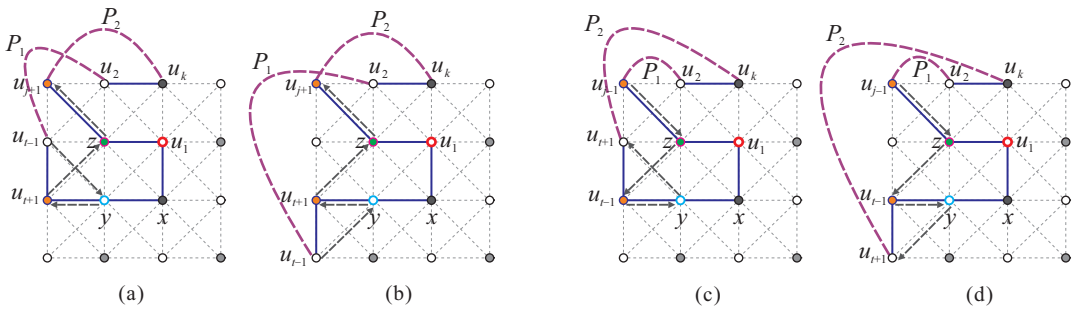

Fig. 17: The construction of extended cycle C' for (a)–(b) Case 1.1 of Claim 1 under the case of Fig. 16(a), and (c)–(d) Case 1.2 of Claim 1 under the case of Fig. 16(a), where solid lines indicate the edges in C', bold dashed lines represent the subpaths of cycle C, and dashed arrow lines indicates edges in C.

(C1) that if $z \nsim x$ then none of $Z \cap V(G)$ is adjacent to x. By inspection on every case of Fig. 12, the possible relative positions among z, x, u_1, u_2, u_k under $z \nsim x$ are shown in Fig. 22. For example, in inspecting the case of Fig. 12(c), by Proposition 2.5 $z = L(u_1) \sim x$ since $UL(u_1) = u_2$ and $DL(u_1) = x$ are in $V(G)$. On the other hand, for the case of 12(d) we get that $z = R(u_1)$. Then, the case is the same as the case of exchanging the positions of u_2 and u_k, and hence $z \sim x$. The other cases can be inspected by the symmetry and linearly convexity of graphs.

We first consider the case of Fig. 22(b). Since $DL(u_1) = x$ and $DR(u_1) = u_k$ are in G, we get $D(u_1) \in V(G)$ by Proposition 2.5. By symmetry, we can exchange u_2 and u_k. Replace $z = R(u_1)$ with $z = D(u_1)$. Then, $z \sim x$ and it can be proved by the similar arguments in proving Claim 1.

Now, we consider the case of Fig. 22(a). We will construct a cycle C' by the similar construction of Claim 1. Since G is 2-connected and linearly convex, at least one of $UR(u_1)$ and $DL(u_1)$ is in G. Suppose that $UR(u_1)$ is in G. By Proposition 2.5, $R(u_1) \in V(G)$. By symmetry, we can exchange the locations of u_2 and u_k. Let $z = R(u_1)$. Then, $z \sim x$, $z \sim u_2$, and it is the case of Fig. 13(a). Thus, an extended cycle C' from C and x can be constructed.

In the following, assume that $UR(u_1) \notin V(G)$. Then, $DL(u_1) \in V(G)$. Since $DL(u_1) \in V(G)$ and $DR(u_1)(= x) \in V(G)$, we get that $D(u_1) \in V(G)$ by Proposition 2.5. Let $y = D(u_1)$. Then, $y \sim z$, $y \nsim u_2$, and $y \nsim u_k$. By the case of Fig. 13(b) in Claim 1, $y \in C$. Let $y = u_t$. Then, $3 \leqslant t \leqslant k-1$. By Proposition 2.1, $x \nsim u_{t-1}$ and $x \nsim u_{t+1}$. Then, $u_{t-1}, u_{t+1} \in \{L(y), DL(y), UL(y)(= z)\}$. Since $(u_1, u_2) \in C$, $z \sim u_1$, and $z \sim u_2$, we get that $z \in C$ by Proposition 2.1. Let $z = u_j$. Then, $3 \leqslant j \leqslant k-1$. Suppose that $z = u_{t-1}$. Let $C_1 = u_1 \to x \to u_t(= y) \to u_{t-1}(= z) \to u_{t-2} \to u_{t-3} \to \cdots \to u_2$ and let $P_1 = u_{t+1} \to u_{t+2} \to \cdots \to u_{k-1} \to u_k$. Then, $start(P_1)(= u_{t+1}) \sim u_t(= y)$ and $end(P_1)(= u_k) \sim u_{t-1}(= z)$. By Proposition 2.2, C_1 and P_1 can be concatenated into a cycle C' with $V(C') = V(C) \cup \{x\}$. On the other hand, suppose that $z = u_{t+1}$. Then, $C' = u_1 \to x \to u_t(= y) \to u_{t-1} \to u_{t-2} \to \cdots \to u_3 \to u_2 \to u_{t+1}(= z) \to u_{t+2} \to \cdots \to u_{k-1} \to u_k$ is a cycle covering $V(C)$ and x, and hence C' is the extension of C. In the following, assume that $z \neq u_{t-1}$ and $z \neq u_{t+1}$. Then, $u_{t-1}, u_{t+1} \in \{L(y), DL(y)\}$ and, hence, $u_{t-1} \sim u_{t+1}$. Depending on whether y appears before z in C, there are two cases as follows.

Case 1: $2 \leqslant j \leqslant t-2$. In this case, y appears after z in C. Suppose that $u_{j-1} \sim u_{j+1}$. We have that $u_{t-1} \sim u_{t+1}$, $z \sim u_2$, and $u_t(= y) \sim u_j(= z)$. Let $C' = u_1 \to x \to u_t(= y) \to u_j(= z) \to u_2 \to u_3 \to \cdots \to u_{j-1} \to u_{j+1} \to u_{j+2} \to \cdots \to u_{t-1} \to u_{t+1} \to u_{t+2} \to \cdots \to u_{k-1} \to u_k$. Then, C' is a Hamiltonian cycle of $G[V(C) \cup \{x\}]$. In the following, suppose that $u_{j-1} \nsim u_{j+1}$. Then, $\{u_{j-1}, u_{j+1}\} = \{UL(z), DL(z)\}$ or $\{UL(z), D(z)\}$. We can see that $D(z) \in \{u_{t-1}, u_{t+1}\}$ and $1 \geqslant |\{u_{j-1}, u_{j+1}\} \cap \{u_{t-1}, u_{t+1}\}| \geqslant 0$. Consider that $\{u_{j-1}, u_{j+1}\} \cap \{u_{t-1}, u_{t+1}\} = \emptyset$. Then, $\{u_{j-1}, u_{j+1}\} = \{UL(z), DL(z)\}$ and $\{u_{t-1}, u_{t+1}\} = \{L(y), DL(y)\}$. Let $C = u_1 \to u_2 \to P_1 \to z(= u_j) \to u_{j+1} \to P_2 \to y(= u_t) \to P_3 \to u_k$, where $end(P_1) = u_{j-1}$, $end(P_2) = u_{t-1}$, and $start(P_3) = u_{t+1}$. Depending on the related positions among $u_{j-1}, u_{j+1}, u_{t-1}, u_{t+1}$, there are four possible locations of vertices and subpaths in C, as shown in Fig. 23(a)–(d). For instance, in Fig. 23(a), $u_{j-1} = UL(z)$, $u_{j+1} = DL(z)$, $u_{t-1} = L(y)$, and $u_{t+1} = DL(y)$. For the cases of Fig. 23(a)–(d), we can construct an extending cycle C' from C to cover x, as in Fig. 23(e)–(h), respectively.

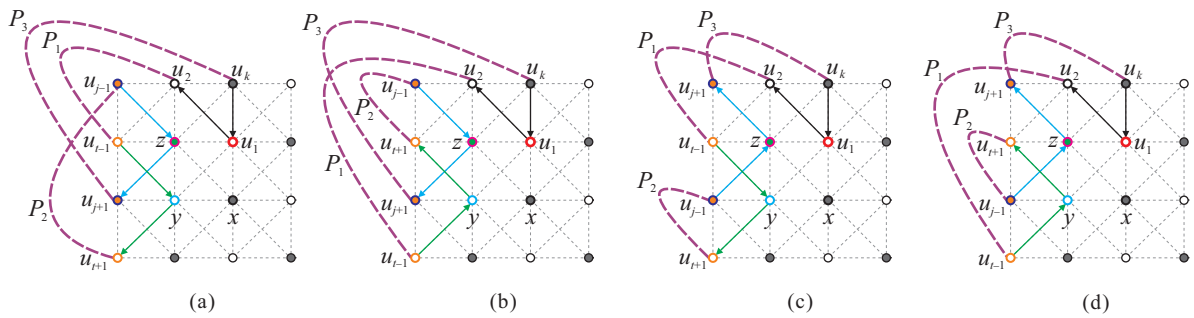

Fig. 18: The possible cycles C for Case 2.1 of Claim 1 under the case of Fig. 16(a), where y appears before z in C, arrow lines indicate the edges in C, and bold dashed lines represent the subpaths of cycle C.

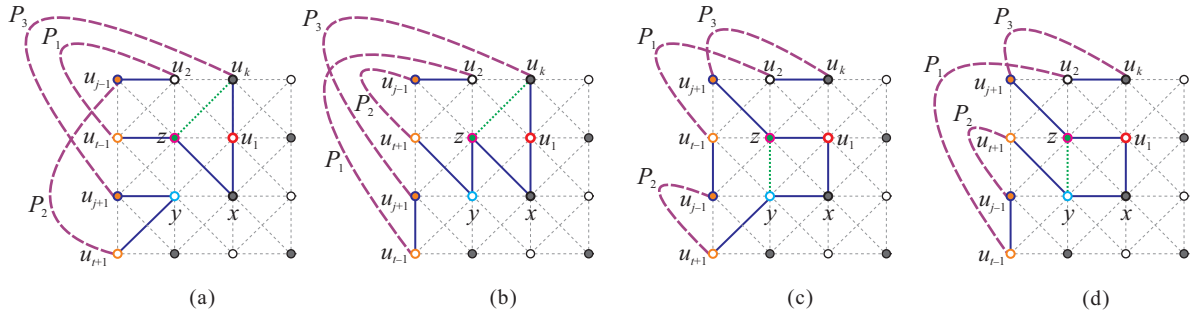

Fig. 19: The constructed extending cycles for Fig. 18(a)–(d), respectively, where dashed dark lines represent subpaths of C, solid lines indicate the edges in the constructed cycle, and dotted line indicate the edge in the immediate cycle C_1 that is incident to edge (u_1, x).

For instance, consider the case of Fig. 23(a), let $C' = u_1 \to x \to y \to P_3 \to u_k \to u_2 \to P_1 \to z \to u_{j+1} \to P_2$, as in Fig. 23(e). Fig. 23(f)–(h) depict the constructed cycles for Fig. 23(b)–(d), respectively. On the other hand, consider that $\{u_{j-1}, u_{j+1}\} \cap \{u_{t-1}, u_{t+1}\} \neq \emptyset$. Then, $\{u_{j-1}, u_{j+1}\} \cap \{u_{t-1}, u_{t+1}\} = D(z) = L(y)$ and an extending cycle C' can be constructed by the similar construction.

Case 2: $t+1 \leqslant j \leqslant k-1$. In this case, y appears before z in C. By similar arguments in proving Case 1, this case can be proved. Consider that $u_{j-1} \sim u_{j+1}$. Then, $C' = u_1 \to x \to u_t(= y) \to u_j(= z) \to u_2 \to u_3 \to \cdots \to u_{t-1} \to u_{t+1} \to u_{t+2} \to \cdots \to u_{j-1} \to u_{j+1} \to u_{j+2} \to \cdots \to u_{k-1} \to u_k$ is a cycle extended from C to cover x. Suppose that $u_{j-1} \nsim u_{j+1}$ below. By the same arguments in proving Case 1, we first consider that $\{u_{j-1}, u_{j+1}\} \cap \{u_{t-1}, u_{t+1}\} = \emptyset$. The possible cycles C and x are shown in Fig. 24(a)–(d). Fig. 24(e)–(h) depict the constructed cycles for the cases of Fig. 24(a)–(d), respectively. On the other hand, consider that $\{u_{j-1}, u_{j+1}\} \cap \{u_{t-1}, u_{t+1}\} \neq \emptyset$. Then, $\{u_{j-1}, u_{j+1}\} \cap \{u_{t-1}, u_{t+1}\} = D(z) = L(y)$. In our construction of cycles in Fig. 24(e)–(g), they contain edge $(DL(z), L(y))$. Thus, we can view this edge as one vertex $D(z)$ and construct the extending cycle C' for the case of $\{u_{j-1}, u_{j+1}\} \cap \{u_{t-1}, u_{t+1}\} \neq \emptyset$. By similar technique, it can be applied to the construction of C' for Fig. 24(h) under that $\{u_{j-1}, u_{j+1}\} \cap \{u_{t-1}, u_{t+1}\} = \{D(z) = L(y)\}$.

We have considered all cases under $z \nsim x$ to show that C is cycle extendable. This completes the proof of Claim 2.□

It immediately follows from Theorem 4.1 that the following theorem holds true.

Theorem 4.2. *Let G be a 2-connected, linear-convex supergrid graph. Then, G contains a Hamiltonian cycle.*

5 Concluding remarks

The Hamiltonian cycle and Hamiltonian path problems for supergrid graphs were known to be NP-complete. In this paper, we first show that 2-connected, linear-convex supergrid graphs are locally connected. We then prove that 2-connected, linear-convex supergrid graphs are cycle extendable and hence are Hamiltonian. It is interesting to see whether the Hamiltonian problems for the other subclasses of supergrid graphs, including solid and locally connected, are polynomial solvable. We would like to post it as an open problem to interested readers.

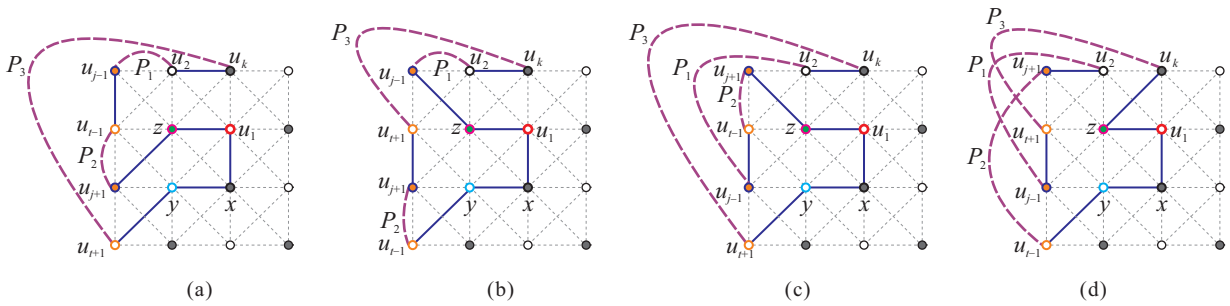

Fig. 20: The constructed cycles C' for Case 2.2 of Claim 1 under the case of Fig. 16(a), where y appears after z in C, arrow lines indicate the edges in C, and bold dashed lines represent the subpaths of cycle C.

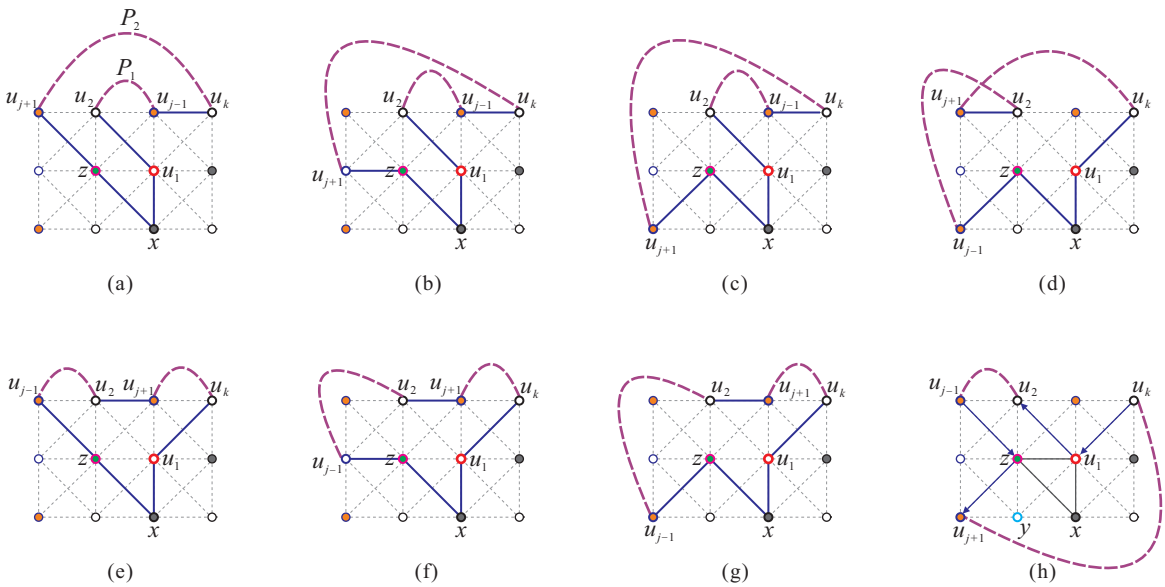

Fig. 21: The possible locations of u_{j-1} and u_{j+1} for the case of Fig. 16(c).

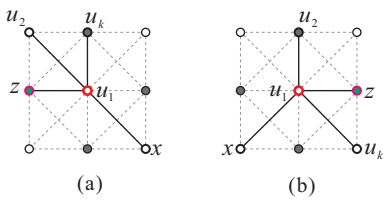

Fig. 22: The possible locations among z, x, u_1, u_2, u_k for Claim 2 with $z \nsim x$.

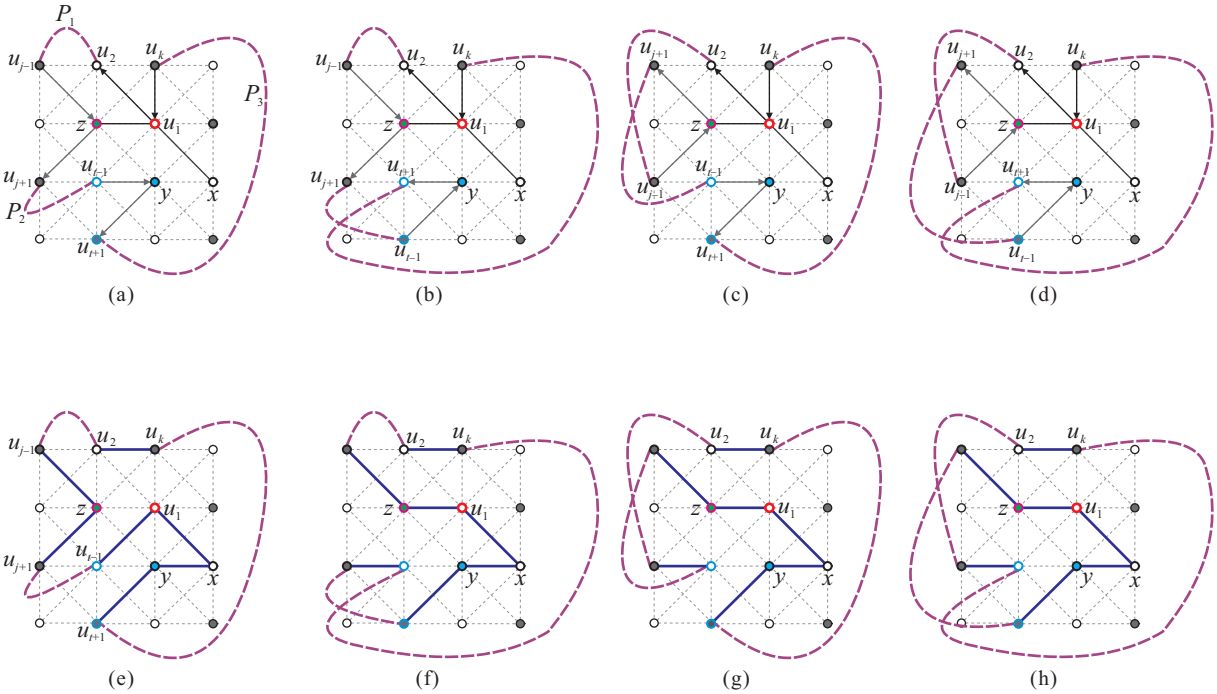

Fig. 23: (a)–(d) The possible cycle C under that $z \nsim x$, $z \notin \{u_{t-1}, u_{t+1}\}$, $2 \leqslant j \leqslant t-2$, $u_{j-1} \nsim u_{j+1}$, and $\{u_{j-1}, u_{j+1}\} \cap \{u_{t-1}, u_{t+1}\} = \emptyset$, where arrow solid lines indicate the edges in C and dark dashed lines represent subpaths of C; (e)–(h) the constructed extending cycle C' containing $V(C)$ and x for (a)–(d), respectively.

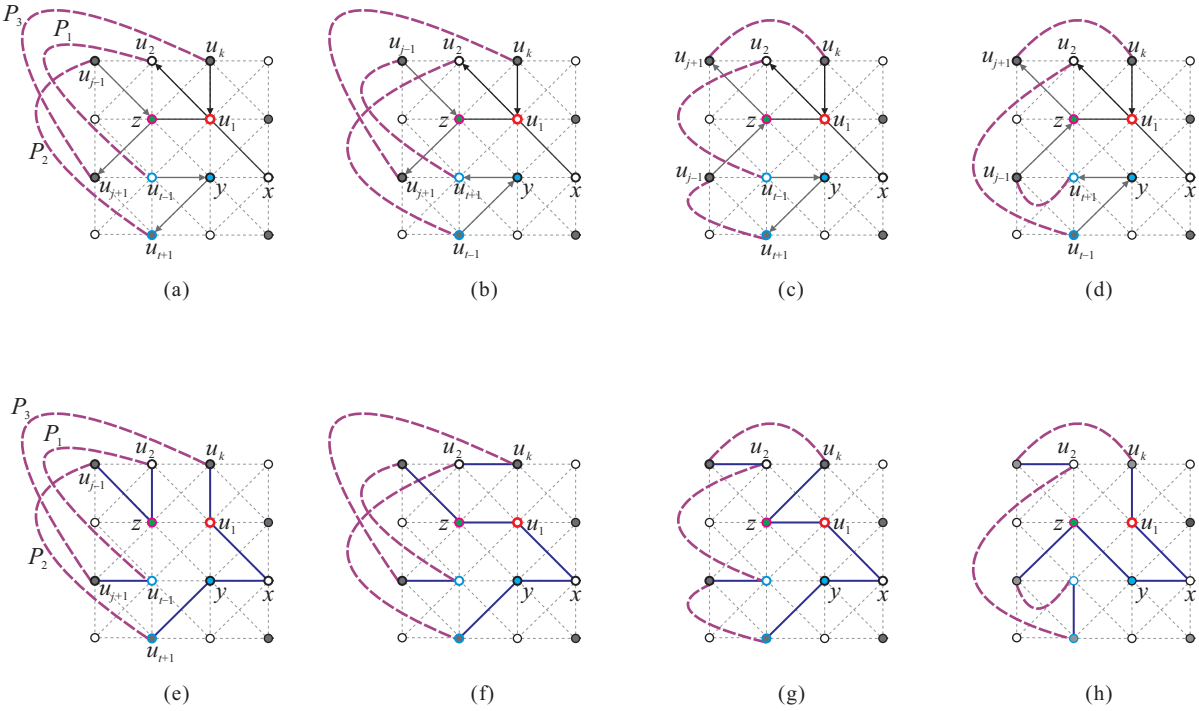

Fig. 24: (a)–(d) The possible cycle C under that $z \nsim x$, $z \notin \{u_{t-1}, u_{t+1}\}$, $t+1 \leqslant j \leqslant k-1$, $u_{j-1} \nsim u_{j+1}$, and $\{u_{j-1}, u_{j+1}\} \cap \{u_{t-1}, u_{t+1}\} = \emptyset$, where arrow solid lines indicate the edges in C and dark dashed lines represent subpaths of C; (e)–(h) the constructed extending cycle C' containing $V(C)$ and x for (a)–(d), respectively.

References

[1] N. Ascheuer, Hamiltonian path problems in the on-line optimization of flexible manufacturing systems, Technique Report TR 96-3, Konrad-Zuse-Zentrum für Informationstechnik, Berlin, 1996.

[2] J.C. Bermond, Hamiltonian graphs, in Selected Topics in Graph Theory ed. by L.W. Beinke and R.J. Wilson, Academic Press, New York, 1978.

[3] A.A. Bertossi, M.A. Bonuccelli, Hamiltonian circuits in interval graph generalizations, Inform. Process. Lett. 23 (1986) 195–200.

[4] J.A. Bondy, U.S.R. Murty, Graph Theory, 2nd Ed., Springer, New York, 2008.

[5] I. Bouchemakh, M. Zemir, On the broadcast independence number of grid graph, Graph. Combinator. 30 (2014) 83–100.

[6] S.D. Chen, H. Shen, R. Topor, An efficient algorithm for constructing Hamiltonian paths in meshes, Parallel Comput. 28 (2002) 1293 – 1305.

[7] P. Damaschke, The Hamiltonian circuit problem for circle graphs is NP-complete, Inform. Process. Lett. 32 (1989) 1–2.

[8] M. Dettlaff, M. Lemańskaa, I.G. Yero, Bondage number of grid graphs, Discrete Appl. Math. 167 (2014) 94–99.

[9] R.J. Faudree, E. Flandrin, Z. Ryjáček, Claw-free graphs - A survey, Discrete Math. 164 (1997) 87–147.

[10] M.R. Garey, D.S. Johnson, Computers and Intractability: A Guide to the Theory of NP-Completeness, Freeman, San Francisco, CA, 1979.

[11] M.C. Golumbic, Algorithmic Graph Theory and Perfect Graphs, Second edition, Annals of Discrete Mathematics 57, Elsevier, 2004.

[12] V.S. Gordon, Y.L. Orlovich, F. Werner, Hamiltonin properties of triangular grid graphs, Discrete Math. 308 (2008) 6166–6188.

[13] S. Gravier, Total domination number of grid graphs, Discrete Appl. Math. 121 (2002) 119–128.

[14] V. Grebinski, G. Kucherov, Reconstructing a Hamiltonian cycle by querying the graph: Application to DNA physical mapping, Discrete Appl. Math. 88 (1998) 147–165.

[15] P. Gulak, T. Kailath, Locally connected VLSI architectures for the Viterbi algorithm, IEEE J. Sel. Areas Commun. 6(3) (1988) 527–537.

[16] G.R.T. Hendry, Extending cycles in graphs, Discrete Math. 85 (1990) 59–72.

[17] F.T. Hu, Y. Lu, J.M. Xu, The total bondage number of grid graphs, Discrete Appl. Math. 160 (2012) 2408–2418.

[18] R.W. Hung, C.C. Yao, S.J. Chan, The Hamiltonian properties of supergrid graphs, Submitted.

[19] K. Islam, H. Meijer, Y. Núñez, D. Rappaport, H. Xiao, Hamiltonian cycles in hexagonal grid graphs, in: Proceedings of the 19th Canadian Conference on Computational Geometry, CCCG'97, 2007, pp. 85–88.

[20] A. Itai, C.H. Papadimitriou, J.L. Szwarcfiter, Hamiltonian paths in grid graphs, SIAM J. Comput. 11(4) (1982) 676–686.

[21] D.S. Johnson, The NP-complete column: an ongoing guide, J. Algorithms 6 (1985) 434–451.

[22] F. Keshavarz-Kohjerdi, A. Bagheri, Hamiltonian paths in some classes of grid graphs, J. Appl. Math. 2012 (1982) article no. 475087.

[23] F. Keshavarz-Kohjerdi, A. Bagheri, A. Asgharian-Sardroud, A linear-time algorithm for the longest path problem in rectangular grid graphs, Discrete Appl. Math. 160 (2012) 210–217.

[24] M.S. Krishnamoorthy, An NP-hard problem in bipartite graphs, SIGACT News 7 (1976) 26.

[25] W. Lenhart, C. Umans, Hamiltonian cycles in solid grid graphs, in: Proceedings of the 38th Annual Symposium on Foundations of Computer Science, FOCS'97, 1997, pp. 496–505.

[26] D. Marx, Eulerian disjoint paths problem in grid graphs is NP-complete, Discrete Appl. Math. 143 (2004) 336–341.

[27] B. Menke, T. Zamfirescu, C. Zamfirescu, Intersections of longest cycles in grid graphs, J. Graph Theory 25 (1997) 37–52.

[28] S. Muthammai, P. Vidhya, Total complementary tree domination in grid graphs, Intern. J. Math. Soft Comput. 3 (2013) 107–114.

[29] J.F. O'Callaghan, Computing the perceptual boundaries of dot patterns, Comput. Graphics Image Process. 3 (1974) 141–162.

[30] F.P. Preperata, M.I. Shamos, Computational Geometry: An Introduction, Springer, New York, 1985.

[31] J.R. Reay, T. Zamfirescu, Hamiltonian cycles in T-graphs, Discrete Comput. Geom. 24 (2000) 497–502.

[32] A.N.M. Salman, Contributions to Graph Theory, Ph.D. thesis, University of Twente, 2005.

[33] G.T. Toussaint, Pattern recognition and geometrical complexity, in: Proceedings of the 5th International Conference on Pattern Recognition, Miami Beach, 1980, pp. 1324–1347.

[34] C. Zamfirescu, T. Zamfirescu, Hamiltonian properties of grid graphs, SIAM J. Disc. Math. 5 (1992) 564–570.

[35] W.Q. Zhang, Y.J. Liu, Approximating the longest paths in grid graphs, Theoret. Comput. Sci. 412 (2011) 5340–5350.